Title

Impact of oviductal versus ovarian epithelial cell of origin on ovarian endometrioid carcinoma phenotype in the mouse

Permalink

Journal

ISSN

Authors

Wu, Rong
Zhai, Yali
Kuick, Rork
et al.

Publication Date

DOI

Peer reviewed

Impact of oviductal versus ovarian epithelial cell of origin on ovarian endometrioid carcinoma phenotype in the mouse

Rong Wu[a,†], **Yali Zhai**[a,†], **Rork Kuick**[b], **Anthony N. Karnezis**[c], **Paloma Garcia**[a], **Anum Naseem**[a], **Tom C. Hu**[a], **Eric R. Fearon**[a,d,e], and **Kathleen R. Cho**[a,d,*]

[a]Department of Pathology, University of Michigan Medical School, 1506 BSRB, 109 Zina Pitcher Place, Ann Arbor, MI, 48109

[b]Department of Biostatistics, University of Michigan School of Public Health, M4509 SPH II, 1415 Washington Heights, Ann Arbor, MI, 48109

[c]Department of Pathology and Laboratory Medicine, University of British Columbia, Vancouver, BC, Canada

[d]Department of Internal Medicine, University of Michigan Medical School, 1506 BSRB, 109 Zina Pitcher Place, Ann Arbor, MI, 48109

[e]Department of Human Genetics, University of Michigan Medical School, 1506 BSRB, 109 Zina Pitcher Place, Ann Arbor, MI, 48109

Abstract

Endometrioid carcinoma (EC) is a relatively indolent ovarian carcinoma subtype that is nonetheless deadly if detected late. Existing genetically engineered mouse models (GEMMs) of the disease, based on transformation of ovarian surface epithelium (OSE), take advantage of known ovarian EC driver gene lesions but do not fully recapitulate disease features seen in patients. An EC model in which the *Apc* and *Pten* tumour suppressor genes are conditionally deleted in murine OSE yields tumours that are biologically more aggressive and significantly less differentiated than human ECs. Importantly, OSE is not currently thought to be the cell of origin of most ovarian cancers, including ECs, suggesting that tumour initiation in Müllerian epithelium may produce tumours more closely resembling their human tumour counterparts. We have developed *Ovgp1-iCreER^{T2}* mice in which the *Ovgp1* promoter controls expression of tamoxifen (TAM)-regulated Cre recombinase in oviductal epithelium – the murine equivalent of human Fallopian tube epithelium. *Ovgp1-iCreER^{T2};Apc^{fl/fl};Pten^{fl/fl}* mice treated with TAM or injected with adenovirus expressing Cre into the ovarian bursa uniformly develop oviductal or ovarian ECs,

*Correspondence to: Kathleen R. Cho, 1506 BSRB, 109 Zina Pitcher Place, University of Michigan, Ann Arbor, MI 48109. Phone, 734-764-1549. kathcho@umich.edu.
†equal contribution

respectively. Based on their morphology and global gene expression profiles, the oviduct-derived tumours more closely resemble human ovarian ECs than do OSE-derived tumours. Furthermore, mice with oviductal tumours survive much longer than their counterparts with ovarian tumours. The slow progression and late metastasis of oviductal tumours resembles the relatively indolent behaviour characteristic of so-called Type I ovarian carcinomas in humans, for which EC is a prototype. Our studies demonstrate the utility of *Ovgp1-iCreER^{T2}* mice for manipulating genes of interest specifically in the oviductal epithelium, and establish that the cell of origin is an important consideration in mouse ovarian cancer GEMMs.

INTRODUCTION

Ovarian carcinomas are sub-classified into different histologic types based on their morphological similarity to the different types of Müllerian epithelium lining the female genital tract. Increasingly, genetic and immunohistochemical signatures help to define ovarian cancer subtypes [1]. Endometrioid carcinoma (EC) is the second most common type of ovarian carcinoma, representing 7–24% of cases [2,3]. Ovarian ECs are characterized by well-formed glands that resemble endometrial glands during the proliferative phase of the menstrual cycle. Most are believed to arise from the Müllerian epithelium associated with endometriosis or benign neoplasms known as endometrioid adenofibromas and endometrioid borderline tumours.

Based on both histopathological and molecular data, a "dualistic" model has been proposed in which ovarian carcinomas can be divided into two main categories that reflect their pathogenetic features [4,5]. Type I ovarian carcinomas are low-grade, relatively indolent and genetically stable tumours, often arising from recognizable precursor lesions, and frequently harbouring somatic mutations that deregulate specific cell signalling pathways or chromatin remodelling complexes. Endometrioid, clear cell, and mucinous carcinomas, and low-grade serous carcinomas are considered Type I tumours. In contrast, Type II carcinomas (mostly high-grade serous carcinomas) are high-grade, biologically aggressive tumours from their outset, with a propensity for metastasis from small-volume primary lesions. Type I tumours have a more favourable prognosis than the Type II tumours, largely because they are more likely to be detected and resected before they have metastasized. However, women with advanced-stage Type I carcinomas have poor overall survival, and more effective therapies are needed [6].

Histologic type-specific models that reflect the heterogeneity of ovarian carcinomas could be used to improve our understanding of their biology and to investigate new prevention strategies, improve early detection, and test novel therapies. Several genetically engineered mouse models (GEMMs) of ovarian EC have been developed based on neoplastic transformation of the ovarian surface epithelium (OSE) instigated by genetic lesions in the murine homologues of genes mutated in human ECs. For example Dinulescu et al generated

a model of EC based on conditional inactivation of *Pten* and activation of *Kras* in the OSE by injecting adenovirus expressing Cre recombinase (AdCre) into the ovarian bursal cavity [7]. Similarly, Guan et al reported a model of EC based on conditional inactivation of *Pten* and *Arid1a* in the OSE [8]. Human ovarian ECs often harbour mutations predicted to concomitantly activate the canonical Wnt and PI3K/AKT signalling pathways [9,10]. We previously described a mouse EC model in which these two pathways are dysregulated by conditional deletion of the *Apc* and *Pten* tumour suppressor genes in the OSE induced by ovarian bursal injection of AdCre [9]. Following concurrent *Apc* and *Pten* inactivation, these mice uniformly and rapidly develop ovarian carcinomas with some similarities to human ECs, although the tumours are significantly less differentiated and behave more aggressively than their human tumour counterparts. The previously described mouse models of ovarian EC arising from OSE transformation have limitations because recent studies suggest that many, perhaps most, ovarian carcinomas do not arise from the OSE. Indeed, Kurman and colleagues have proposed that both Type I and Type II ovarian carcinomas typically involve the ovaries as a metastatic site, or arise from extra-ovarian Müllerian cells that involve the ovary secondarily [11,12].

Carcinomas with endometrioid differentiation comprise the majority of uterine endometrial cancers, and can also arise in the fallopian tube, albeit uncommonly [13–17]. We have developed mice in which the *Ovgp1* (oviductal glycoprotein 1) promoter is used to drive expression of tamoxifen (TAM)-regulated Cre recombinase specifically in the oviductal (equivalent to human Fallopian tube) epithelium, and not in the OSE. In this study, we wished to study effects of cell of origin on the morphological and biological features of tumours arising from Müllerian epithelium vs. the OSE. *Ovgp1-iCreER^{T2}* mice harbouring floxed *Apc* and *Pten* alleles were treated with TAM to induce oviductal tumour formation. Tumours were also induced in the OSE of genetically comparable mice by injecting AdCre into the ovarian bursal cavities. Our goal was to determine which of the two model systems yields tumours that better recapitulate the morphological features, gene expression profiles, and biological behaviour of human ovarian EC.

MATERIALS AND METHODS

Genetically modified mice and animal care

To generate *Ovgp1-iCreER^{T2}* transgenic mice, a codon-improved *iCreER^{T2}* cDNA was inserted at the translation initiation codon of *Ovgp1* within a 90 kb bacterial artificial chromosome (BAC) (RP23-169-H9) containing the entire *Ovgp1* locus, using the Counter Selection BAC Modification Kit (Gene Bridge, Heidelberg, Germany). Recombinant BAC DNA was microinjected into fertilized (C57BL/6 X SJL) F2 mouse eggs (University of Michigan Transgenic Animal Model Core) as described by Nagy et al [18]. Selected founder lines were crossed with reporter mice carrying the *Gt(ROSA)26Sor^{tm1(EYFP)Cos}*/J allele (hereafter referred to as *Rosa^{LSL-EYFP}*) (Jackson laboratory, Bar Harbor, ME, USA) to generate *Ovgp1-iCreER^{T2};Rosa^{LSL-EYFP}* double transgenic mice. The *Ovgp1-iCreER^{T2}* mice were also crossed with *Apc^{fl/fl};Pten^{fl/fl}* mice to generate triple transgenic *Ovgp1-iCreER^{T2};Apc^{fl/fl};Pten^{fl/fl}* mice. The *Apc^{fl/fl};Pten^{fl/fl}* mice have been described previously in detail [9,19,20]. All strains were maintained on a mixed genetic background, and littermates

were used for the *Ovgp1-iCreER^{T2}* and AdCre gene targeting. Procedures involving mice for the research described herein have been approved by the University of Michigan's Institutional Animal Care and Use Committee (PRO00006370).

Induction of oviductal and ovarian tumours

Ovgp1-iCreER^{T2} female mice were given intraperitoneal (IP) injections of TAM (Sigma-Aldrich, Indianapolis, IN,) to activate Cre in the oviductal (murine Fallopian tube) epithelium (hereafter referred to as FTE). TAM was dissolved in corn oil (Sigma Aldrich) and injected at 0.1g/kg of body weight twice (day 1 and day 3) when mice were 6–8 weeks old. Alternatively, *Ovgp1-iCreER^{T2};Apc^{fl/fl};Pten^{fl/fl}* mice were injected with 5×10^7 p.f.u. of replication-incompetent AdCre into both ovarian bursal cavities for ovarian tumour formation as previously described [9].

Histopathology, immunohistochemistry, and immunofluorescence

Mice were grossly inspected for tumour location and extent at necropsy. Ovaries, oviducts, uteri, lungs, kidneys, liver, omentum, and mesentery were examined microscopically in each case. Tissues were fixed in formalin and paraffin-embedded. Sections were H&E-stained for evaluation by light microscopy. Immunohistochemistry (IHC) was performed on formalin-fixed paraffin-embedded tissue sections using standard methods. Antigen retrieval was performed by microwaving the slides in citrate buffer (pH 6.0; Biogenex, San Ramon, CA) for 15 minutes. Endogenous peroxidase activity was quenched with 6% hydrogen peroxide in methanol. Staining was visualized with 3,3′-diaminobenzidine tetrahydrochloride and counterstaining with haematoxylin. Primary antibodies used were rat anti-cytokeratin 8 (TROMA I, 1:100, Developmental Studies Hybridoma Bank, University of Iowa), mouse anti β-catenin (cat# 610154, 1:500, Transduction Laboratories, Lexington, KY), rabbit anti-PTEN (138G6/cat#9559, 1:400, Cell Signaling Technology, Inc., Danvers, MA), rabbit anti-PAX8 (cat# 10336-1-AP, 1:500, Proteintech, Chicago, IL), and goat anti-OVGP1 (cat# 10336-1-AP, 1:500, Santa Cruz Biotechnology, Inc., Santa Cruz, CA). For immunofluorescence (IF) staining, tissues were fixed with 4% paraformaldehyde at room temperature and then embedded in paraffin. Deparaffinized sections were permeabilized with PBS containing 0.5% Triton X-100 for 10 min, blocked with PBS containing 5% normal goat serum for one hour and then incubated with primary rabbit anti-GFP (cat# 10336-1-AP, 1:500, Cell Signaling) and rabbit anti-tubulin (cat# T6199, 1:1000, Sigma-Aldrich) antibodies at 4 °C overnight. After washing with PBS, slides were incubated with secondary goat anti-rabbit IgG conjugated with FITC 488 (for GFP), and goat anti-rabbit IgG conjugated with Alexa 594 Red (for tubulin) for one h at room temperature. Sections were mounted with Prolong Gold antifade reagent (Thermo Fisher Scientific, Waltham, MA).

Gene expression analyses

Affymetrix Mouse Gene 2.1 ST Plate Arrays were used to profile gene expression in six FTE-derived mouse oviductal tumours and five OSE-derived ovarian tumours. Four normal whole ovary samples from *Ovgp1-iCreER^{T2};Apc^{fl/fl};Pten^{fl/fl}* mice that had not been injected with either AdCre or TAM were also profiled (each sample representing a pool of two normal ovaries per mouse). Total RNA was extracted from manually dissected frozen mouse

tumour samples using adjacent H&E-stained sections as dissection guides, in order to ensure that each tumour sample contained at least 90% tumour cells and lacked significant necrosis. RNA was extracted using Trizol (Invitrogen), and purified using RNeasy columns (Qiagen). Quality was checked with an Agilent 2100 Bioanalyzer. Total RNA (250–400 ng) was reverse-transcribed, amplified and labelled using Affymetrix PLUS kits. Following fragmentation, cDNA was hybridized for 20 h at 48 °C to Mouse Genome 2.1 ST arrays. Arrays were scanned using the Affymetrix Gene Atlas system. Transcript abundances were estimated using the Robust Multi-Array Average (RMA) algorithm [21] using Bioconductor software in the R-statistical programming environment. It reports log2-transformed abundances and subsequent analyses used the log-transformed data for 25216 probe-sets associated with mouse gene identifiers in the annotation obtained from Bioconductor. Principal component analysis was carried out and an ANOVA (Analysis of Variance) model was used to identify differentially expressed genes between each pair of groups. Gene expression data from 99 human ovarian carcinomas to which the mouse tumor data were compared, have been previously described in detail and are available from the NCBI's Gene Expression Omnibus (GEO) using series accession number GSE6008 [9]. Mouse genes were mapped to human gene IDs by using 1-to-1 best homologs from build 68 of Homologene, yielding a total of 15813 distinct human genes. The mouse gene expression data reported here are also available from the GEO (accession number GSE80085).

Results

Cre activation is limited to the oviductal epithelium in TAM-treated *Ovgp1-iCreER^T2* mice

In order to assess the *Ovgp1* promoter's suitability for directing Cre expression specifically in the FTE of adult mice, IHC was first used to assess endogenous OVGP1 protein expression in selected normal mouse tissues (Figure 1). Strong OVGP1 expression was found in the FTE but OVGP1 expression was absent in the ovary (including the OSE), liver, lung, pancreas, spleen, and lymph node. Endometrial glandular epithelium in the portion of the uterine horns adjacent to the oviduct and tubules in the kidney occasionally showed focal weak OVGP1 staining. To generate mice allowing conditional (ligand-regulated) expression of Cre recombinase in the FTE, a BAC containing the mouse *Ovgp1* locus was engineered to include a cassette encoding Cre fused to a ligand-binding domain sequence of human *ESR1* (oestrogen receptor) and the *BGH* polyadenylation signal sequence. The cassette was inserted at the translation initiation codon in the first exon of *Ovgp1*. Recombinant BAC DNA was microinjected into fertilized embryos by standard pronuclear injection techniques. Several transgenic founders were shown to yield viable and fertile male and female transgenic offspring. All of the *Ovgp1-iCreER^T2* mice employed in this study were derived from the same founder.

To demonstrate the specificity of Cre recombinase function in the FTE, *Ovgp1-iCreER^T2* mice were crossed with *Rosa^LSL-EYFP* reporter mice to generate double transgenic *Ovgp1-iCreER^T2;Rosa^LSL-EYFP* animals. Double transgenic female mice were injected with TAM or vehicle (corn oil) and euthanized one week after the second injection. Major organs were collected and examined using a stereo fluorescent microscope. Representative tissues were examined by IF microscopy. EYFP expression was detected only in the oviducts of TAM-

treated *Ovgp1-iCreER^{T2};Rosa^{LSL-EYFP}* mice (Figure 2A), but not vehicle-treated *Ovgp1-iCreER^{T2};Rosa^{LSL-EYFP}* mice (Figure 2B). EYFP fluorescence was similarly absent in the oviducts of vehicle or TAM-treated *Ovgp1-iCreER^{T2}* transgene-negative mice (not shown). To determine which oviductal epithelial cells (secretory vs. ciliated) express EYFP we carried out double IF analyses using an anti-GFP antibody and an anti-tubulin antibody, as tubulin is expressed by ciliated cells. In TAM-treated *Ovgp1-iCreER^{T2};Rosa^{LSL-EYFP}* mice, EYFP is primarily expressed in oviductal secretory cells and not in ciliated cells (Figure 2C,D). EYFP expression was not seen in other major organs, including the ovary, uterus, liver, lung, pancreas, kidney, spleen, lymph node, and brain (not shown).

Conditional bi-allelic inactivation of *Apc* and *Pten* in FTE results in oviductal carcinomas that closely resemble human ovarian ECs

We crossed *Ovgp1-iCreER^{T2}* mice with *Apc^{fl/fl};Pten^{fl/fl}* mice to generate triple transgenic *Ovgp1-iCreER^{T2};Apc^{fl/fl};Pten^{fl/fl}* animals. Cohorts of 6–8 week old females were treated with TAM and euthanized at regular intervals to monitor tumour development and progression (Table 1). Early changes (oviductal epithelial hyperplasia and atypia) were observed starting ~1 month after TAM injection and primarily affected the infundibular (comparable to human fimbriae) and ampullary (mid) portions of the oviducts. By 9–12 weeks post-TAM, mice developed well-formed oviductal EC-like tumours. The endometrium and ovaries showed no detectable alterations at comparable time points. Representative photomicrographs of EC arising in the oviducts of TAM-treated mice over time are shown in Figure 3A and Supplementary Figure S1. Fifteen mice with oviductal ECs were followed for 16–33 weeks post TAM. Tumours involved the ovaries (often extensively) in 10 mice, and a subset of these also had metastases to the omentum (n=4) or lungs (n=1). Grossly, tumours varied in size from 2 to 6mm in diameter. Microscopically, the tumours were well to moderately differentiated adenocarcinomas with overt gland formation, closely resembling human ovarian ECs (Figure 3A). Based on the FIGO (International Federation of Gynecology and Obstetrics) criteria used for grading human ovarian ECs, eleven of the mouse oviductal tumours would be classified as grade 1 (5% solid growth) and four as grade 2 (5–50% solid growth). None were classified as grade 3 (> 50% solid growth). As expected, the oviductal tumours expressed cytokeratin 8 and PAX8, and showed nuclear/cytoplasmic staining for β-catenin and loss of PTEN expression (Figure 3C). Metastases were also CK8 and PAX8 positive, supporting origin from an oviductal primary (Supplementary Figure S1).

Conditional bi-allelic inactivation of *Apc* and *Pten* in the OSE of genetically comparable mice results in poorly differentiated ovarian carcinomas

In order to compare effects of bi-allelic inactivation of *Apc* and *Pten* in the FTE vs. OSE, AdCre was injected into the ovarian bursae of *Ovgp1-iCreER^{T2};Apc^{fl/fl};Pten^{fl/fl}* mice from the same founder line. This approach allows a direct comparison of tumours arising from Müllerian epithelial (FTE) transformation, to those arising from OSE in mice with a nearly identical genetic background. AdCre-injected mice uniformly developed tumours by 5 weeks after AdCre administration, in accordance with our previous data [9,22]. Tumour-bearing mice rapidly reached humane endpoints for tumour burden and were euthanized no later than 14 wk following AdCre injection. The OSE-derived tumours (OSE-ECs) were

much larger (10–15mm in diameter at 6–14 wk post AdCre) than the FTE-derived tumours (FTE-ECs) (2–6mm in diameter at 10–33 wk post TAM). Microscopically, the OSE-ECs were very poorly differentiated (all grade 3 based on FIGO criteria), with sparse glandular elements admixed with prominent spindle cell areas (Figure 3A). Compared to the FTE-ECs, the OSE-ECs showed much less CK8 expression and did not express PAX8 (Figure 3C). Like the oviductal tumours, the ovarian tumours expressed nuclear and cytoplasmic β-catenin and lacked PTEN expression. Importantly, the difference in overall survival of AdCre-injected (n=12) versus TAM-treated mice (n=13) was quite striking (61 d vs 193 d median survival, respectively, P=1E-7) (Figure 3B). Overall survival of the AdCre injected mice was even shorter than we previously reported [9,23], perhaps because we performed bilateral bursal injections of AdCre in the current study, in contrast to our prior work in which only unilateral bursal injection was performed.

Global gene expression in mouse oviductal ECs more closely resembles human ovarian carcinomas than mouse ovarian ECs

We profiled gene expression in six FTE-ECs, five OSE-ECs and four normal ovary (NO) mouse samples using Affymetrix Mouse ST 2.1 Arrays. This array approach was selected so we could more easily compare gene expression in the mouse tumours to human tumour data collected previously with a comparable platform. The normal ovary samples for these experiments simply serve as a common reference point for comparing gene expression in tumours from mouse and human, respectively, as comparable hybridization of mouse and human cRNAs to probe sets representing homologous genes in the mouse and human cannot be assumed. Principal component analysis showed that the mouse oviductal and ovarian tumours were about as dissimilar to each other as when oviductal or ovarian tumours were compared to normal controls (Supplementary Figure S2). An ANOVA model was used to identify differentially expressed genes between pairs of groups. About 3 000 probe-sets (of 25 216) gave p<0.001 and fold-changes greater than 2 for pairwise comparisons of any two groups, with false discovery rates of less than 0.5% (see Supplementary Table S1 and details provided in our GEO submission). A heat map showing the top 80 differentially expressed genes between the oviductal and ovarian *Apc-/Pten-* mouse tumours is provided in Supplementary Figure S3. Although the oviductal and ovarian tumours were based on the same genetic defects (bi-allelic *Apc* and *Pten* inactivation), tumours arising from the two sites differed in the expression of many putative Wnt signalling-regulated target genes (Supplementary Table S2) as well as for expression of genes in other pathways.

To determine whether the oviductal or ovarian mouse tumours more closely resemble human ovarian carcinomas, we correlated the individual tumour versus average normal differences with similar tumour versus normal differences in our previous human array data from 4 normal ovaries and 99 ovarian carcinomas (37 endometrioid, 41 serous, 13 mucinous and 8 clear cell), using 10 727 genes reported to be 1-to-1 best homologs by NCBI's Homologene. For each gene we selected the probe-set that gave the smallest p-value for overall F-test comparing groups within each species (3 groups for mouse, 5 for human). We initially believed correlating T-statistics might be better than merely correlating the distances (in log space) since this performs well as an enrichment testing technique [24]; however, we obtained nearly identical results, and report on the simpler distances. We fit the model

Rijkm= Uik +Aij +Bkm +Eijkm where Rijkm is the correlation of the j-th mouse from the i-th mouse group with the m-th human from the k-th human group. The Uik are the averages for the i-th mouse group and the k-th human group, which can be compared using F-tests coming from the model. Aij and Bkm are terms for each mouse and human - a highly idiosyncratic human tumour is likely to give lower correlations for every mouse tumour, and *vice versa*. Figure 4A demonstrates the expected variation between individual human and mouse tumours, and importantly, shows that mouse oviductal tumours were more correlated as a group to every class of human ovarian carcinomas than mouse ovarian tumours ($p<10^{-60}$). Only 2 of the 99 human tumours were more correlated to mouse OSE-ECs than to mouse FTE-ECs (Figure 4B). Correlations using all genes are modest, since expression of most genes are unaltered between normal and tumour tissues and/or between tumour groups. For our human OE samples we had previous mutation and IHC expression data for *CTNNB1*/β-catenin (Figure 4A) [9]. A comparison of 14 OEs with mutant *CTNNB1* and/or nuclear expression of β-catenin to 23 OEs with wild-type *CTNNB1* showed significantly higher correlations in the *CTNNB1* mutant group (means 0.240 and 0.212, $P = 0.004$). Mouse oviductal tumours were more correlated to human endometrioid carcinomas and mucinous carcinomas than to clear cell and serous carcinomas on average ($p <3\times10^{-7}$ in each possible pairwise comparison). Average correlations between mouse and human tumours are shown in Supplementary Table S3, with differences between FTE-ECs versus OSE-ECs to each group of human tumours being highly significant. In short, mouse tumours derived from FTE transformation have gene expression profiles much more closely related to human ovarian carcinomas (especially endometrioid carcinomas with *CTNNB1* mutations) than to mouse tumours that arise from transformed OSE.

Discussion

Potential non-ovarian origins of ovarian carcinomas have been the focus of much discussion and debate, and several reviews have emphasized the need for better model systems with which to gain mechanistic insights into the genetic, biologic, and physiologic factors that contribute to ovarian tumour development and progression [25–27]. Many GEMMs of ovarian cancer have been reported, most based on transformation of the OSE [see [28] for recent review]. Indeed, nearly all of the Type I ovarian carcinoma GEMMs reported to date, including prior work from our group, employ either the *Amhr2* promoter or injection of AdCre into the ovarian bursa to drive Cre-mediated recombination in the OSE [7–9,23,29–33]. Interestingly, van der Horst and colleagues recently employed the *Pgr* (progesterone receptor) promoter to drive Cre-mediated inactivation of *Apc* in Müllerian epithelium, including the endometrium and oviduct. These mice develop endometrial hyperplasia and oviductal intraepithelial lesions and carcinomas as well as ovarian ECs proposed to arise from ovarian inclusion cysts and glands [34]. Though we are fully aware that the majority of human "ovarian" ECs are not thought to arise from the Fallopian tube, neither do they likely arise from the OSE. The studies described herein support the notion that cell of origin has profound effects on the phenotype of tumours induced by the same genetic defects. Moreover, transformation of Müllerian epithelium such as the FTE, leads to tumours that more closely resemble human ovarian carcinomas than do comparable tumours arising in the murine OSE.

Particular gene defects or combinations of defects may have cell-of-origin and tissue-specific effects on cell phenotypes, perhaps providing key insights into the origin of different histological subtypes of ovarian carcinomas. For instance, conditional inactivation of *Brca1* and *Trp53* in the murine OSE often leads to the development of leiomyosarcomas [35,36], which is not detected following induction of the same genetic alterations in the mouse FTE [37]. More recently, studies employing syngeneic murine oviductal and OSE allografts have also shown that the same genetic alterations in different cell types can give rise to different cancer histotypes [38]. Here we present data showing distinctive effects of *Apc* and *Pten* loss in the FTE compared to OSE *in vivo*. Specifically, ovarian bursal injection of AdCre in *Ovgp1-iCreERT2;Apc^{fl/fl};Pten^{fl/fl}* mice results in rapid OSE transformation and the development of poorly-differentiated carcinomas. In contrast, when *Apc* and *Pten* loss is induced in the FTE, well-differentiated tumours develop over months rather than weeks. Mouse oviductal tumours were more correlated than mouse ovarian tumours to every class of human ovarian carcinomas, with highest correlation to human endometrioid and mucinous carcinomas. While the similarity to human endometrioid carcinomas (particularly those with *CTNNB1* mutations) was expected, the similarity to human mucinous carcinomas was unanticipated and remains incompletely understood. However, both are considered Type I tumours and human endometrioid carcinomas have a known propensity to display foci of mucinous differentiation, a feature that was also observed in some of the mouse oviductal, but not ovarian tumours.

Tissue-specific effects of *Apc* and *Pten* loss are highlighted by some striking differences in expression of Wnt signalling pathway targets in the oviductal versus ovarian *Apc-/Pten-* tumours. For example, *Mmp7* and *Sox9* are much more highly overexpressed in the oviductal tumours than the ovarian tumours while the converse is true for *Ccnd1, Fgf20,* and *Klf5. Lgr5,* a putative marker of stem/progenitor cells in ovary and tubal epithelia [39,40], is upregulated only in the oviductal tumours. Interestingly, *Ctnnb1* is up-regulated in tumours from both sites, supporting our prior work providing evidence for a feed-forward role for β-catenin in canonical Wnt signalling [41].

Ovgp1 encodes a protein that is secreted by non-ciliated cells in mammalian FTE [42]. OVGP1 appears to play a role in optimizing the microenvironment for oocyte maturation and transport, fertilization, and early embryonic development [43]. Although maximum production of OVGP1 has been shown to be dependent on plasma oestrogen level in cows, baboon, sheep, pigs and humans, this does not appear to be the case in rabbits or hamsters [44]. We did not need to pre-treat our *Ovgp1-iCreER^{T2}* mice with oestradiol prior to treating them with TAM in order to strongly activate Cre in the oviductal epithelium. In 2002, Miyoshi et al described the development of high-grade serous carcinoma-like tumours arising in transgenic mice expressing SV40 Large T-Ag under control of a 2.2kb fragment of the murine *Ovgp1* promoter [45]. Lesions arising in these mice were more recently described in detail [46]. In addition to oviductal tumours and presumptive metastases to the ovaries, epithelial and mesenchymal malignant lesions also developed in the uteri of older mice. Importantly, we did not observe endometrial carcinoma or uterine sarcoma in any of our *Ovgp1-iCreER^{T2};Apc^{fl/fl};Pten^{fl/fl}* mice monitored for up to 33 wk post-TAM treatment. Thus, our *Ovgp1-iCreER^{T2}* mice provide an excellent system with which to test effects of various genetic alterations specifically in the FTE.

Our findings provide compelling evidence that depending on the specific tissues targeted for transformation, the same combination of genetic alterations leads to very different tumour phenotypes. Comparable studies testing other combinations of gene mutations common in EC, as well as effects of gene combinations characteristic of HGSC are in progress and will help establish whether models based on transformation of Müllerian (e.g., oviductal) epithelium will prove more suitable than those derived from OSE for studying ovarian cancer biology and for translational applications.

Supplementary Material

Refer to Web version on PubMed Central for supplementary material.

Acknowledgments

References

1. Kobel M, Kalloger SE, Lee S, et al. Biomarker-based ovarian carcinoma typing: a histologic investigation in the ovarian tumor tissue analysis consortium. Cancer Epidemiol Biomarkers Prev. 2013; 22:1677–1686. [PubMed: 23880734]

2. Seidman JD, Horkayne-Szakaly I, Haiba M, et al. The histologic type and stage distribution of ovarian carcinomas of surface epithelial origin. Int J Gynecol Pathol. 2004; 23:41–44. [PubMed: 14668549]

3. Gilks CB, Ionescu DN, Kalloger SE, et al. Tumor cell type can be reproducibly diagnosed and is of independent prognostic significance in patients with maximally debulked ovarian carcinoma. Hum Pathol. 2008; 39:1239–1251. [PubMed: 18602670]

4. Shih, IeM; Kurman, RJ. Ovarian tumorigenesis: a proposed model based on morphological and molecular genetic analysis. Am J Pathol. 2004; 164:1511–1518. [PubMed: 15111296]

5. Kurman RJ, Shih IeM. Pathogenesis of ovarian cancer: lessons from morphology and molecular biology and their clinical implications. Int J Gynecol Pathol. 2008; 27:151–160. [PubMed: 18317228]

6. Braicu EI, Sehouli J, Richter R, et al. Role of histological type on surgical outcome and survival following radical primary tumour debulking of epithelial ovarian, fallopian tube and peritoneal cancers. Br J Cancer. 2011; 105:1818–1824. [PubMed: 22045193]

7. Dinulescu DM, Ince TA, Quade BJ, et al. Role of K-ras and Pten in the development of mouse models of endometriosis and endometrioid ovarian cancer. Nat Med. 2005; 11:63–70. [PubMed: 15619626]

8. Guan B, Rahmanto YS, Wu RC, et al. Roles of deletion of Arid1a, a tumor suppressor, in mouse ovarian tumorigenesis. J Natl Cancer Inst. 2014:106.

9. Wu R, Hendrix-Lucas N, Kuick R, et al. Mouse model of human ovarian endometrioid adenocarcinoma based on somatic defects in the Wnt/B-catanin and PI3K/Pten signaling pathways. Cancer Cell. 2007; 11:321–333. [PubMed: 17418409]

10. McConechy MK, Ding J, Senz J, et al. Ovarian and endometrial endometrioid carcinomas have distinct CTNNB1 and PTEN mutation profiles. Mod Pathol. 2014; 27:128–134. [PubMed: 23765252]

11. Kuhn E, Kurman RJ, Shih IM. Ovarian Cancer Is an Imported Disease: Fact or Fiction? Curr Obstet Gynecol Rep. 2012; 1:1–9. [PubMed: 22506137]

12. Kurman RJ, Shih Ie M. Molecular pathogenesis and extraovarian origin of epithelial ovarian cancer-Shifting the paradigm. Hum Pathol. 2011; 42:918–931. [PubMed: 21683865]

13. Rorat E, Wallach RC. Endometrioid carcinoma of the fallopian tube: pathology and clinical outcome. Int J Gynaecol Obstet. 1990; 32:163–167. [PubMed: 1972104]

14. Alvarado-Cabrero I, Young RH, Vamvakas EC, et al. Carcinoma of the fallopian tube: a clinicopathological study of 105 cases with observations on staging and prognostic factors. Gynecol Oncol. 1999; 72:367–379. [PubMed: 10053109]

15. Huang W, Zhao Y, Zhao J, et al. Endometrioid carcinoma of the fallopian tube resembling an adnexal tumor of probable wolffian origin: a case of report and review of the literature. Pathol Res Pract. 2010; 206:180–184. [PubMed: 19457622]

16. Navani SS, Alvarado-Cabrero I, Young RH, et al. Endometrioid carcinoma of the fallopian tube: a clinicopathologic analysis of 26 cases. Gynecol Oncol. 1996; 63:371–378. [PubMed: 8946874]

17. Culton LK, Deavers MT, Silva EG, et al. Endometrioid carcinoma simultaneously involving the uterus and the fallopian tube: a clinicopathologic study of 13 cases. Am J Surg Pathol. 2006; 30:844–849. [PubMed: 16819326]

18. Nagy, A.; Gertsenstein, M.; Vintersten, K., et al. Manipulating the Mouse Embryo: A Laboratory Manual. Cold Spring Harbor Press; New York: 2003.

19. Shibata H, Toyama K, Shioya H, et al. Rapid colorectal adenoma formation initiated by conditional targeting of the Apc gene. Science. 1997; 278:120–123. [PubMed: 9311916]

20. Suzuki A, Yamaguchi MT, Ohteki T, et al. T cell-specific loss of Pten leads to defects in central and peripheral tolerance. Immunity. 2001; 14:523–534. [PubMed: 11371355]

21. Irizarry RA, Hobbs B, Collin F, et al. Exploration, normalization, and summaries of high density oligonucleotide array probe level data. Biostatistics. 2003; 4:249–264. [PubMed: 12925520]

22. Wu R, Hu T, Rehemtulla A, et al. Preclinical Testing of PI3K/AKT/mTOR Signaling Inhibitors in a Mouse Model of Ovarian Endometrioid Adenocarcinoma. Clin Cancer Res. 2011; 17:7359–7372. [PubMed: 21903772]

23. Wu R, Baker SJ, Hu TC, et al. Type I to Type II Ovarian Carcinoma Progression: Mutant Trp53 or Pik3ca Confers a More Aggressive Tumor Phenotype in a Mouse Model of Ovarian Cancer. Am J Pathol. 2013; 182:1391–1399. [PubMed: 23499052]

24. Shedden K. Confidence levels for the comparison of microarray experiments. Stat Appl Genet Mol Biol. 2004; 3 Article32.

25. Auersperg N. Ovarian surface epithelium as a source of ovarian cancers: unwarranted speculation or evidence-based hypothesis? Gynecol Oncol. 2013; 130:246–251. [PubMed: 23558054]

26. Dubeau L, Drapkin R. Coming into focus: the nonovarian origins of ovarian cancer. Ann Oncol. 2013; 24(Suppl 8):viii28–viii35. [PubMed: 24131966]

27. Perets R, Drapkin R. It's Totally Tubular…Riding The New Wave of Ovarian Cancer Research. Cancer Res. 2016; 76:10–17. [PubMed: 26669862]

28. Committee on the State of the Science in Ovarian Cancer Research BoHCS, Institute of Medicine; National Academies of Sciences, Engineering, and Medicine. National Academy of Sciences. Ovarian Cancers: Evolving Paradigms in Research and Care. 2016.

29. Fan HY, Liu Z, Paquet M, et al. Cell type-specific targeted mutations of Kras and Pten document proliferation arrest in granulosa cells versus oncogenic insult to ovarian surface epithelial cells. Cancer Res. 2009; 69:6463–6472. [PubMed: 19679546]

30. Mullany LK, Fan HY, Liu Z, et al. Molecular and functional characteristics of ovarian surface epithelial cells transformed by KrasG12D and loss of Pten in a mouse model in vivo. Oncogene. 2011; 30:3522–3536. [PubMed: 21423204]

31. Zhai Y, Kuick R, Tipton C, et al. Arid1a inactivation in an Apc- and Pten-defective mouse ovarian cancer model enhances epithelial differentiation and prolongs survival. J Pathol. 2015

32. Tanwar PS, Zhang L, Kaneko-Tarui T, et al. Mammalian target of rapamycin is a therapeutic target for murine ovarian endometrioid adenocarcinomas with dysregulated Wnt/beta-catenin and PTEN. PLoS One. 2011; 6:e20715. [PubMed: 21695255]

33. Chandler RL, Damrauer JS, Raab JR, et al. Coexistent ARID1A-PIK3CA mutations promote ovarian clear-cell tumorigenesis through pro-tumorigenic inflammatory cytokine signalling. Nature communications. 2015; 6:6118.

34. van der Horst PH, van der Zee M, Heijmans-Antonissen C, et al. A mouse model for endometrioid ovarian cancer arising from the distal oviduct. Int J Cancer. 2014; 135:1028–1037. [PubMed: 24474556]

35. Quinn BA, Brake T, Hua X, et al. Induction of ovarian leiomyosarcomas in mice by conditional inactivation of Brca1 and p53. PLoS One. 2009; 4:e8404. [PubMed: 20046879]

36. Clark-Knowles KV, Senterman MK, Collins O, et al. Conditional inactivation of Brca1, p53 and Rb in mouse ovaries results in the development of leiomyosarcomas. PLoS One. 2009; 4:e8534. [PubMed: 20046869]

37. Perets R, Wyant GA, Muto KW, et al. Transformation of the fallopian tube secretory epithelium leads to high-grade serous ovarian cancer in brca;tp53;pten models. Cancer Cell. 2013; 24:751–765. [PubMed: 24332043]

38. Eddie SL, Quartuccio SM, EOh, et al. Tumorigenesis and peritoneal colonization from fallopian tube epithelium. Oncotarget. 2015; 6:20500–20512. [PubMed: 25971410]

39. Flesken-Nikitin A, Hwang CI, Cheng CY, et al. Ovarian surface epithelium at the junction area contains a cancer-prone stem cell niche. Nature. 2013; 495:241–245. [PubMed: 23467088]

40. Ng A, Tan S, Singh G, et al. Lgr5 marks stem/progenitor cells in ovary and tubal epithelia. Nat Cell Biol. 2014; 16:745–757. [PubMed: 24997521]

41. Feng Y, Sakamoto N, Wu R, et al. Tissue-Specific Effects of Reduced beta-catenin Expression on Adenomatous Polyposis Coli Mutation-Instigated Tumorigenesis in Mouse Colon and Ovarian Epithelium. PLoS genetics. 2015; 11:e1005638. [PubMed: 26528816]

42. Natraj U, Bhatt P, Vanage G, et al. Overexpression of monkey oviductal protein: purification and characterization of recombinant protein and its antibodies. Biol Reprod. 2002; 67:1897–1906. [PubMed: 12444068]

43. Buhi WC. Characterization and biological roles of oviduct-specific, oestrogen-dependent glycoprotein. Reproduction. 2002; 123:355–362. [PubMed: 11882012]

44. Aviles M, Gutierrez-Adan A, Coy P. Oviductal secretions: will they be key factors for the future ARTs? Mol Hum Reprod. 2010; 16:896–906. [PubMed: 20584881]

45. Miyoshi I, Takahashi K, Kon Y, et al. Mouse transgenic for murine oviduct-specific glycoprotein promoter-driven simian virus 40 large T-antigen: tumor formation and its hormonal regulation. Mol Reprod Dev. 2002; 63:168–176. [PubMed: 12203826]

46. Sherman-Baust CA, Kuhn E, Valle BL, et al. A genetically engineered ovarian cancer mouse model based on fallopian tube transformation mimics human high-grade serous carcinoma development. J Pathol. 2014; 233:228–237. [PubMed: 24652535]
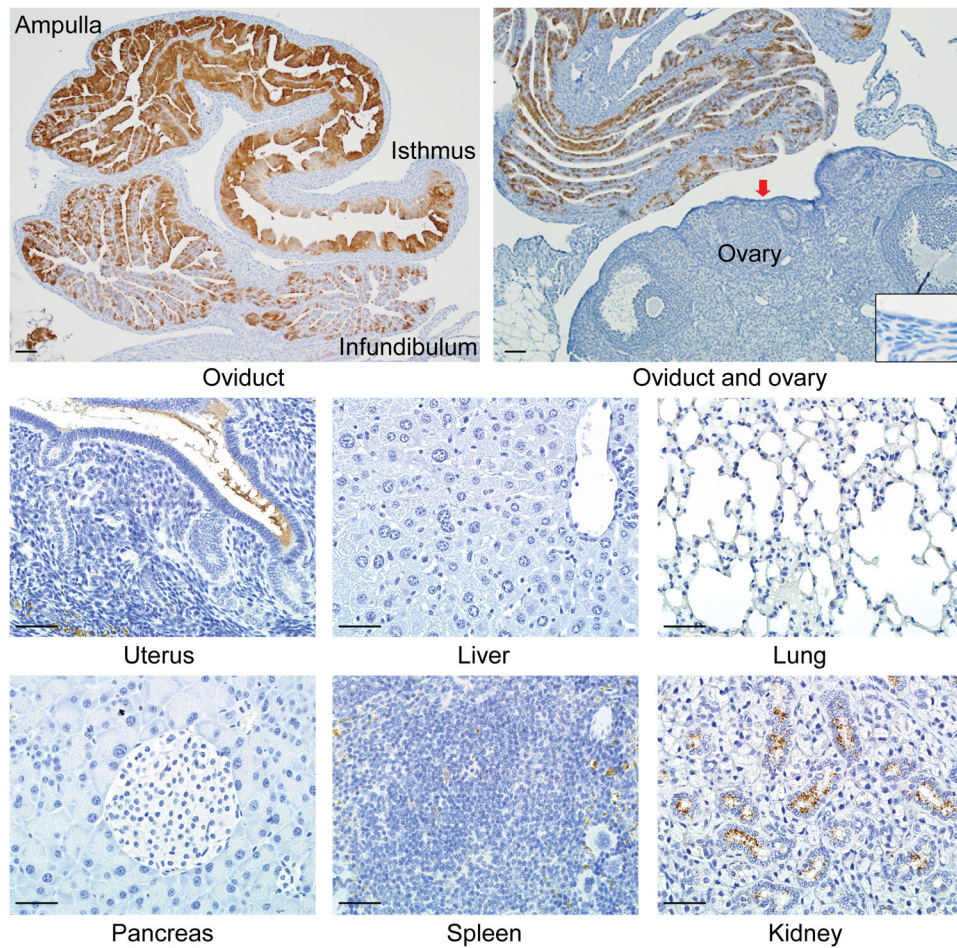
Figure 1. OVGP1 is highly expressed in oviductal epithelium but not in other tissues in the mouse
Representative sections of the adult mouse organs shown were stained using standard immunohistochemical methods and an anti-OVGP1 antibody. Red arrow highlights the absence of OVGP1 expression in the ovarian surface epithelium. Scale bars represent 100 μm.
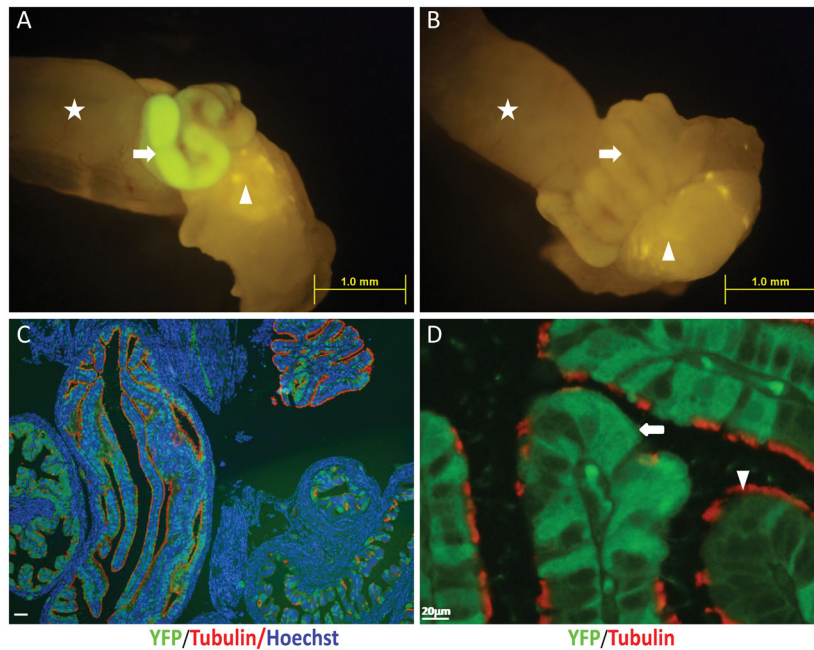
YFP/Tubulin/Hoechst   YFP/Tubulin

Figure 2. Characterization of *Ovgp1-iCreER^{T2}* mice

Oviductal expression of EYFP is induced by TAM **(A)** but not by vehicle **(B)** treatment in double transgenic *Ovgp1-iCreER^{T2};Rosa^{LSL-EYFP}* mice. Mouse oviducts are indicated by white arrows, ovaries by white arrow heads and uterine horns by white stars. The green oviduct is seen in the TAM-treated, but not vehicle-treated mouse (yellow flecks on the ovaries represent autofluorescence). Representative low magnification **(C)** and high magnification **(D)** photomicrographs of double immunofluorescent staining showing YFP (green) and tubulin (red) expression in the oviductal epithelium of TAM-treated *Ovgp1-iCreER^{T2};Rosa^{LSL-EYFP}* mice. EYFP is primarily expressed in non-ciliated secretory cells (representative cell indicated by white arrow) and not in the ciliated cells (representative cell indicated by white arrowhead).
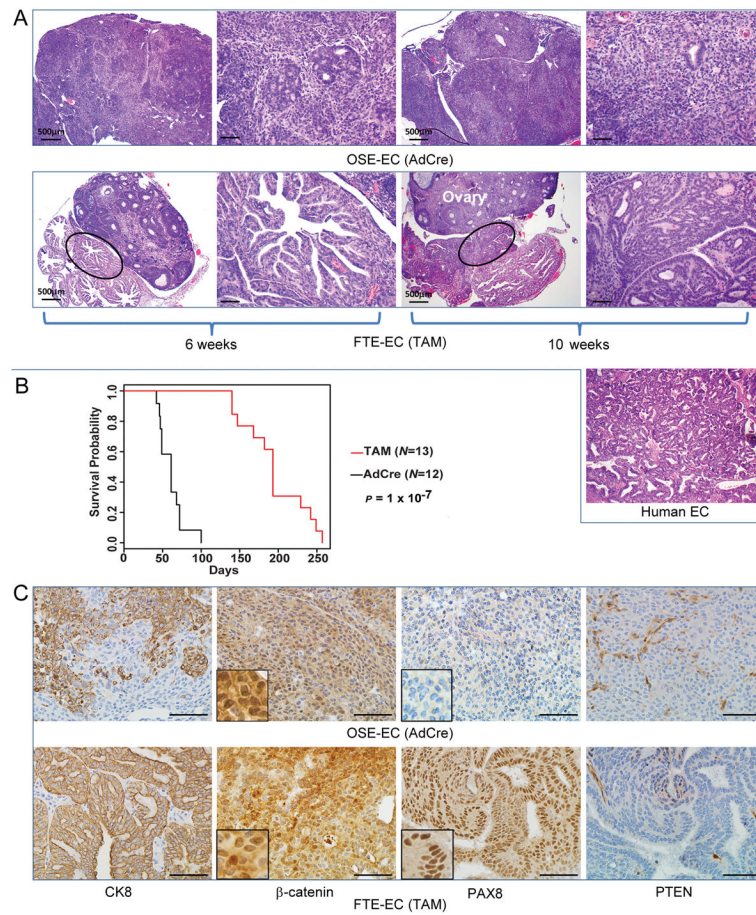
Figure 3. Comparison of OSE- and FTE-derived endometrioid carcinomas in *Ovgp1-iCreER^{T2};Apc^{fl/fl};Pten^{fl/fl}* mice

(**A**) Upper panels show OSE-derived tumours and lower panels show FTE-derived tumors at 6 weeks and 10 weeks after tumour induction with AdCre or TAM respectively. Areas within the ellipses in lower panels indicate oviductal region with EC development. The histological features of a representative human ovarian EC is shown for comparison with the mouse tumors. (**B**) Kaplan-Meier survival curves of tumour-bearing *Ovgp1-iCreER^{T2};Apc^{fl/fl};Pten^{fl/fl}* mice following injection of AdCre (n=12) versus TAM (n=13). (**C**) Immunohistochemical analysis of CK8, β-catenin, PAX8 and PTEN in the OSE- and FTE-derived ECs, as indicated. Boxed areas are shown at higher magnification. Scale bars represent 100 μm, unless otherwise indicated.
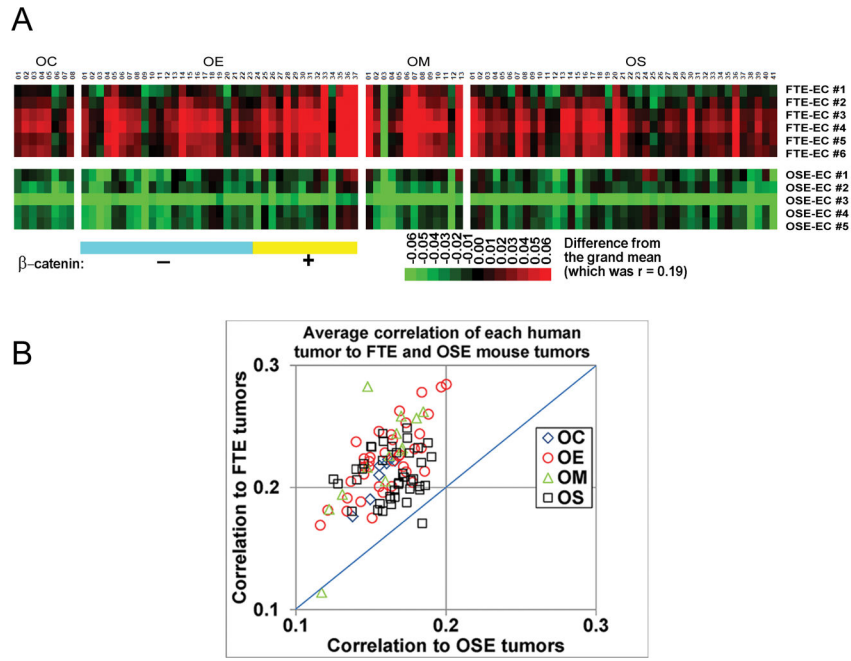
Figure 4. Correlations of mouse FTE-ECs and OSE-ECs to each of 99 human ovarian carcinomas

(A) Heat map showing correlations of individual mouse to human tumours. Each human tumour is annotated as clear cell (OC), endometrioid (OE), mucinous (OM), or serous (OS) carcinoma. Human OEs have been sorted based on the presence (yellow) or absence (blue) of *CTNNB1* mutation and/or nuclear accumulation of β-catenin as indicated. (B) Average correlation of each human tumour to FTE- and OSE-derived mouse tumours.

Table 1

Summary of oviductal EC development in TAM-treated *Ovgp1-iCreER^{T2};Apc^{fl/fl};Pten^{fl/fl}* mice

Weeks post TAM	n	Oviduct			Metastasis		
		FTE Morphology	FIGO grade 1	FIGO grade 2	Ovary	Omentum	Lungs
2–3	2	normal					
4–5	3	epithelial hyperplasia					
6–7	6	epithelial hyperplasia with atypia					
9–12	5	adenocarcinoma	5				
16–33	15	adenocarcinoma	11	4	10	4	1